

Integration within and between muscles during terrestrial locomotion: effects of incline and speed

Timothy E. Higham* and Andrew A. Biewener

Department of Organismic and Evolutionary Biology, Concord Field Station, Harvard University, 100 Old Causeway Road, Bedford, MA 01730, USA

*Author for correspondence (e-mail: thigham@fas.harvard.edu)

Accepted 30 April 2008

SUMMARY

Animals must continually adapt to varying locomotor demands when moving in their natural habitat. Despite the dynamic nature of locomotion, little is known about how multiple muscles, and different parts of a muscle, are functionally integrated as demand changes. In order to determine the extent to which synergist muscles are functionally heterogeneous, and whether this heterogeneity is altered with changes in demand, we examined the *in vivo* function of the lateral (LG) and medial (MG) gastrocnemius muscles of helmeted guinea fowl (*Numida meleagris*) during locomotion on different inclines (level and uphill at 14°) and at different speeds (0.5 and 2.0 m s⁻¹). We also quantified function in the proximal (pMG) and distal (dMG) regions of the MG to examine the extent to which a single muscle is heterogeneous. We used electromyography, sonomicrometry and tendon force buckles to quantify activation, length change and force patterns of both muscles, respectively. We show that the LG and MG exhibited an increase in force and stress with a change in gait and an increase in locomotor speed, but not with changes in incline. While the LG and MG exhibited similar levels of stress when walking at 0.5 m s⁻¹, stress in the LG was 1.8 times greater than in the MG when running at 2.0 m s⁻¹. Fascicle shortening increased with an increase in speed on both inclines for the LG, but only on the level for the pMG. Positive work performed by the LG exceeded that of the pMG and dMG for all conditions, and this difference was magnified when locomotor speed increased. Within the MG, the pMG shortened more, and at a faster rate than the dMG, resulting in a greater amount of positive work performed by the pMG. Mean spike amplitude of the electromyogram (EMG) bursts increased for all muscle locations with an increase in speed, but changes with incline were more variable. The functional differences between the LG and MG are likely due to the different moments each exerts at the knee, as well as differences in motor unit recruitment. The differences within the MG are likely due to motor unit recruitment differences, but also differences in architecture. Fascicles within the dMG insert into an extensive aponeurosis, which results in a higher apparent dynamic stiffness relative to fascicles operating within the pMG. On the level surface, the greater compliance of the pMG leads to increased stretch of its fascicles at the onset of force, further enhancing force production. Our results demonstrate the capacity for functional diversity between and within muscle synergists, which occur with changes in gait, speed and grade.

Key words: synergist, running, locomotion, bird, guinea fowl, bipedal, muscle, sonomicrometry, electromyography, muscle work, muscle strain, dynamic stiffness.

INTRODUCTION

Animal movement is often complex, unsteady and variable. This complexity is driven, in part, by the structural nonuniformity of habitats, which include inclined surfaces and features that cause animals to move at variable speeds. Thus, these factors are important when considering the range of locomotor function in vertebrates. The considerable diversity in locomotor behavior among terrestrial vertebrates is facilitated by the complex functional integration of the limb muscles, which has been recognized for over a century (Pettigrew, 1874; Marey, 1901). Despite this, little is known about how work is distributed among muscles during locomotion, and even less is known about the functional variation within a muscle. Muscle work is commonly assumed to be distributed in proportion to muscle mass (McMahon, 1984; Alexander, 1992; Biewener, 1998), but this assumption has rarely been tested. Understanding the integration between and within muscles will be fundamental for understanding how muscles drive locomotor movements and how muscles adapt to changes in demand.

Moving uphill requires an increased amount of muscle work in order to increase the potential energy of the body with each

stride. This has been studied at the level of whole-body work and energetics (Minetti et al., 1999), as well as within individual limb muscles (Roberts et al., 1997; Daley and Biewener, 2003; Gabaldon et al., 2004; Rubenson et al., 2006). This increased work is facilitated by an increase in motor activation of the limb muscles (Pierotti et al., 1989; Higham and Jayne, 2004a; Wickler et al., 2005; Roberts et al., 2007) and an increase in muscle fascicle strain (Roberts et al., 1997; Daley and Biewener, 2003; Gabaldon et al., 2004; Wickler et al., 2005; McGowan et al., 2007; Roberts et al., 2007). However, not all limb muscles respond similarly to changes in mechanical demand. For example, the lateral gastrocnemius of guinea fowl (ankle extensor) increases its net work output when moving uphill compared with level locomotion, whereas the digital flexor-IV (ankle extensor) does not (Daley and Biewener, 2003). In addition, the mechanical function of individual muscles can be modified in response to changes in incline by altering the timing of muscle activation and force development relative to muscle strain (Gabaldon et al., 2004; Higham and Jayne, 2004a).

Running faster elevates the demand placed on the locomotor system due, in part, to a decreased duty factor, which increases the amount of force required from the limb muscles (Biewener, 2003). In this case, motor unit recruitment, muscle strain and strain rate can all increase (Nelson and Jayne, 2001; Gillis et al., 2005; Wickler et al., 2005; Roberts et al., 2007). Despite the considerable amount of data addressing the effects of speed and incline on muscle function, two important questions that have largely been unexplored are how these changes in mechanical demand are managed by the multiple muscles within different limb regions and whether different regions within a muscle function similarly. One option is that all muscles and regions respond similarly to increases in demand, while another option is that certain muscles exhibit altered function during particular changes in demand (e.g. speed) while other muscles exhibit altered function during other changes (e.g. jumping). Exploring how different muscles, and different regions within a muscle, respond to changes in functional demand will provide insight into how composite structures (i.e. limbs) move.

For a given behavior, muscle synergists can exhibit similar function (Gabaldon et al., 2004), but they can also be functionally decoupled (Herzog and Leonard, 1991; Prilutsky et al., 1996; Ahn and Full, 2002; Higham et al., 2008; Nelson and Roberts, 2008). Differential changes in synergist function in response to a change in motor task have largely been associated with differences in motor unit composition (Walmsley et al., 1978). The same is true for single muscles in that some can act as a homogenous unit (Gillis et al., 2005), while others can exhibit heterogeneous function, such as spatial variation in length change (Pappas et al., 2002; Ahn et al., 2003; Soman et al., 2005; Lichtwark et al., 2007; Higham et al., 2008). Several mechanisms can explain the existence of heterogeneous function within a muscle, including regional differences in force generation (Carrasco et al., 1999), fiber type regionalization (Chanaud et al., 1991; Wang and Kernell, 2000; Mu and Sanders, 2001; Wang and Kernell, 2001), regional variation in motor unit recruitment (English, 1984; Chanaud and Macpherson, 1991; Nelson and Jayne, 2001; Scholle et al., 2001; Higham et al., 2008), non-uniform force-length relationships (Morgan, 1985) and spatial variation in architecture (Pappas et al., 2002; Finni et al., 2003; Higham et al., 2008). It is important to highlight that these mechanisms include active (neural control) and passive (anatomical) factors (Nishikawa et al., 2007). The functional role of heterogeneity within a muscle is poorly understood but is extremely important for understanding how muscles deal with changes in demand and for understanding the overall energy expenditure of a muscle. In addition, musculoskeletal models can be improved by knowing what drives heterogeneity and how different factors contribute to this heterogeneity (Blemker et al., 2007).

As ankle extensors, the lateral (LG) and medial (MG) gastrocnemius muscles provide a substantial contribution to the required muscle force during locomotion (Walmsley et al., 1978; Prilutsky et al., 1996; Higham et al., 2008), and these two muscles receive considerable blood flow during locomotion (Ellerby et al., 2005; Ellerby and Marsh, 2006). Using the LG and MG, we tested the following hypotheses: (1) Muscle synergists, and single muscles, exhibit similar *in vivo* recruitment, force and strain patterns during locomotion and (2) based on recent work (Roberts et al., 2007), changes in incline will have greater effects on muscle strain compared with changes in speed. We measured the *in vivo* activation patterns, length-change patterns, and forces exerted by the LG and MG of helmeted guinea fowl (*Numida meleagris*) via their individual distal tendons at two different speeds and gaits (walk, 0.5 m s^{-1} ; run, 2.0 m s^{-1}) and on two inclines (0° and 14°). In addition, we explored

the functional heterogeneity within the MG by measuring activation patterns (important for understanding the relative timing and magnitude of fiber recruitment within a muscle) and length-change patterns of the muscle's proximal (pMG) and distal (dMG) regions.

MATERIALS AND METHODS

Experimental subjects

Four helmeted guinea fowl (*Numida meleagris* L., French breed) of comparable size (average mass, $2.3 \pm 0.2 \text{ kg}$) were used. This species is ideal for studies of animal locomotion as they are easily trained to run on a treadmill and are capable of maintaining a high level of running performance (Daley and Biewener, 2003; Marsh et al., 2004; Marsh et al., 2006; Higham et al., 2008). All surgical and experimental protocols were approved by the Harvard University Institutional Animal Care and Use Committee.

Surgical protocol

The birds were anesthetized using an intramuscular injection of ketamine (20 mg kg^{-1}) and xylazine (2 mg kg^{-1}). During the surgical procedures, subsequent anesthesia was maintained at 1–2% isoflurane while monitoring the animal's breathing rate. Recording electrodes and transducers were passed subcutaneously to the shank from a 1–2 cm dorsal incision over the synsacrum. A second 4–5 cm incision was then made on the lateral side of the right shank, overlying the division between the anterior and posterior muscular compartments, to expose the LG and its tendon. A third 4–5 cm incision was then made on the medial side of the right shank to expose the MG and its tendon.

Sonomicrometry crystals (2.0 mm; Sonometrics, Inc., London, ON, Canada) were implanted in the proximal and distal regions of the MG and the proximal region of the LG (Fig. 1). Small openings in the muscle (approximately 3 mm deep) were made using fine forceps, and the crystals were placed in these openings such that each crystal pair was aligned along a fascicle axis. The crystals were secured using 4-0 silk suture to close the muscle opening. In all muscles and locations, crystals were spaced approximately 10 mm apart.

Fine-wire (0.1 mm diameter; California Fine Wire, Inc., Grover Beach, CA, USA), twisted, silver bipolar electromyographic (EMG) hook electrodes (0.5 mm bared tips with 1 mm spacing) were implanted using a 24-gauge hypodermic needle immediately adjacent to each pair of sonomicrometry crystals and secured to the muscle's fascia using 4-0 silk suture. Electrodes were implanted into the proximal and distal regions of the LG and MG.

E-type stainless steel tendon buckle force transducers were used as described in previous studies (Biewener et al., 1998; Biewener and Corning, 2001; Daley and Biewener, 2003). Strain gauges attached to the buckles were 0.5 mm long and 1.5 mm wide (type FLA-05-11; TML Tokyo Sokki Kenkyujo Co., Ltd, Tokyo, Japan). Although the MG and LG have separate tendons before joining to form a common tendon of insertion, the size of the buckles required that we separate a short (~5 mm) proximal portion of the common tendon. We did this using a number 10 scalpel blade. Subsequent *post-mortem* inspection revealed no sign of further damage to the tendons as a result of being separated in this fashion. In order to predict regional patterns of work within the MG, measurement of force from the MG tendon required the assumption that all parts of the MG generated equal amounts of force.

All lead wires (from EMG, sonomicrometry and tendon buckles) were pre-soldered to an insulated connector (Newark, Chicago, IL, USA). The connector was wrapped in duct tape and sutured to the skin of the back using 4-0 vicryl. Vetwrap (3M, St Paul, MN, USA) was then used to surround the lead wires and connector.

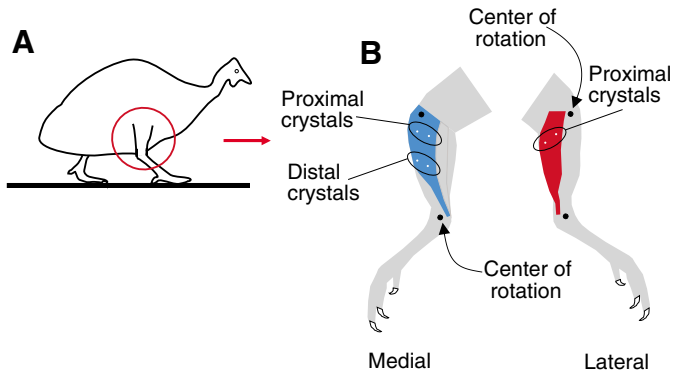


Fig. 1. A diagram showing the location of the muscles relative to the animal's body (A), and the location of the sonomicrometry crystals implanted into the medial gastrocnemius (blue) and the lateral gastrocnemius (red) (B). The center of rotation at the knee (above) and ankle (below) are also shown. Adapted from Higham et al. (Higham et al., 2008).

Experimental protocol

Animals ran on a motorized treadmill at level and uphill (14°) orientations. Although the animals ran over a range of speeds (0.5 to 2.5 ms^{-1}), we chose to analyze data for two speeds (0.5 and 2.0 ms^{-1}) representing a walk and a run, respectively (Gatesy and Biewener, 1991; Gatesy, 1999; Daley and Biewener, 2003). It is important to note that a small subset of the data presented here (force and work values for the two running speeds on the level) was taken from Higham et al. (Higham et al., 2008). Each sequence was recorded in lateral view using a digital high-speed camera (Photron Fastcam 1024PCI; Photron USA Inc., San Diego, CA, USA) at a rate of $250 \text{ frames s}^{-1}$. A trigger (post) stopped the camera recording, and the voltage pulse from the trigger was used to synchronize the video with the *in vivo* muscle data. The order of the trials was randomized between individuals.

Lightweight shielded cable (Cooner Wire, Chatsworth, CA, USA) attached to the connector on the bird's back was attached to a Triton 120.2 sonomicrometry amplifier (Triton Technology Inc., San Diego, CA, USA), a strain gauge bridge amplifier (Vishay 2120; Micromeritics, Raleigh, NC, USA) and EMG amplifiers (P-511; Grass, West Warwick, RI, USA). EMG signals were amplified $2000\times$ and filtered (60 Hz notch, 100–3000 Hz bandpass) before sampling. The outputs of these amplifiers were sampled by an A/D converter (Axon Instruments, Union City, CA, USA) at 5000 Hz . Because the filters in the Triton sonomicrometry unit introduced a 5 ms phase delay, all length measurements were corrected for this offset. Following experiments, animals were euthanized with an intravenous (brachial) injection of sodium pentobarbital (120 mg kg^{-1}).

Force buckle calibration

Immediately following experiments, and after the birds were euthanized, the tendon force buckles were calibrated *in situ* by cutting each muscle at its distal region, in the region of the muscle's aponeurosis attachment to the free tendon, and tying 00 silk sutures around them. The distal attachments of the tendons were left intact, although the tarsometatarsus was removed from the body. The sutured muscle segment was frozen in a shallow dish containing liquid nitrogen and then the suture was tied to a Kistler 9203 force transducer (Amherst, NY, USA). Tension was applied cyclically to the tendon until the loads exceeded the maximum output recorded

in vivo (see Daley and Biewener, 2003). We retrieved a calibration for each buckle using a least-squares linear regression fit to the rise and fall of the buckle output *versus* applied force measured from the force transducer. All buckle calibration regressions yielded r^2 values that were greater than 0.98.

Muscle morphology

Each muscle was dissected free to confirm placement of sonomicrometry crystals and EMG electrodes and to obtain measurements of wet muscle mass, mean fascicle length and pennation angle. This information, assuming a muscle density of 1060 kg m^{-3} , was used to calculate muscle physiological cross-sectional area (PCSA), as in (Powell et al., 1984). Muscle force measurements were converted to muscle stress by dividing force by PCSA.

EMG analysis

EMG recordings for each stride cycle analyzed were first baseline-corrected. Several timing variables were quantified including onset, offset and duration. These timing variables were related to other key events, such as the time of force generation. The rectified integrated area and mean spike amplitude (intensity) were also determined.

Sonomicrometry

Sonomicrometry techniques and analyses followed previous studies (Biewener and Corning, 2001; Daley and Biewener, 2003). Fractional length changes ($\Delta L_{\text{seg}}/L_0$) of the muscle's fascicles were calculated based on segment length changes measured between the crystals (L_{seg}) relative to the resting length (L_0), which was measured while the animal stood at rest. As a convention, shortening strains are negative, and lengthening strains are positive. Total fascicle length change was calculated as fractional length multiplied by the mean fascicle length of the muscle (L_f). Fascicle shortening velocity (muscle lengths per second, $L \text{ s}^{-1}$, or fascicle strain rate) was calculated by dividing the fractional length change during shortening (when force is being produced by the muscle) by the duration of shortening.

Muscle work

Instantaneous changes in muscle fascicle length (corrected for pennation angle) were multiplied by instantaneous force measurements to obtain values of work as a function of time. Values of negative (eccentric contractions) and positive (concentric contractions) work were summed to obtain the positive and negative work done by each muscle and muscle region. The pMG and dMG were assumed to exert similar forces at the muscle's tendon since it is not possible to measure forces from different parts of a muscle. Values of work for a given muscle were divided by muscle mass to obtain mass-specific work.

Apparent dynamic stiffness

Similar to previous studies (Josephson, 1997), we measured dynamic stiffness in the LG, pMG and dMG as the change in force by the change in fascicle length ($=\Delta F/\Delta L_f$). It is important to note, however, that Josephson measured dynamic stiffness to understand how length and stimulation patterns influence the dynamic stiffness of a muscle under *in situ* conditions (Josephson, 1997). In the current study, we are measuring dynamic stiffness under *in vivo* conditions to understand how different regions of a muscle (and different muscles) operate under dynamic conditions. Because we are assuming equal force generation between the pMG and dMG (we only measured

force at the distal tendon), we are calling our measure apparent dynamic stiffness (*ADS*). We measured *ADS* during the force development phase of stance (rise in force). For each muscle region and trial, *ADS* was determined by the following equation:

$$ADS = (\Delta F / |\text{fascicle shortening}|) + (\Delta F / |\text{fascicle lengthening}|) .$$

Statistical analyses

Linear regressions were used to determine the relationships between maximum muscle force and EMG mean spike amplitude for each muscle and region, and the relationships between maximum MG force and maximum LG force. Four-way analyses of variance (ANOVAs) were performed to address the effects of incline and speed on several variables. In these models, individual (random), muscle (fixed) or muscle region (fixed), speed (fixed) and incline (fixed) were the independent variables.

Because the sonomicrometry crystals and EMG electrodes were located at comparable longitudinal locations in the LG and pMG, these two areas were compared to assess the heterogeneity between muscle synergists. To reduce dimensionality, search for axes of correlated variation in muscle function (LG and pMG), and to avoid the error associated with executing multiple statistical tests, 13 variables were included in a principal components analysis (PCA): mean muscle force, maximum muscle force, mean muscle stress, maximum muscle stress, net fascicle strain during force production, EMG duration, force duration, EMG mean spike amplitude, EMG rectified integrated area, the offset between EMG onset and force onset, fascicle strain from force onset to max force, fascicle strain during swing, and fascicle strain from maximum force to the offset of force. These variables have previously been highlighted as important for muscle function (McMahon, 1984; Biewener, 1998). Despite the LG and MG being predominantly stance-phase muscles, a swing variable was included in the PCA since there is often a short period of force generation near the end of swing. The resulting principal components (PC1, PC2 and PC3) became the axes of a multidimensional muscle function space and were visualized in graphical form. To determine if incline and speed occupied different regions of muscle function space, three-way ANOVAs were performed with speed (fixed), incline (fixed) and individual (random) as the independent variables and the PC scores from a particular axis as the dependent variable. A factor loading that was greater than 0.60 was considered a conservative cutoff for significance (Peres-Neto et al., 2003; Higham, 2007).

In order to visualize the regions within the MG in multivariate space, eight variables were included in a PCA: Fascicle strain from the onset of force to maximum force, fascicle strain from maximum force to the offset of force, net fascicle strain during force production, fascicle strain during swing, EMG duration, mean spike amplitude, rectified integrated area, and the offset between EMG onset and

force onset. The number of variables for this analysis (eight) was less than for the LG–pMG comparison (13) because variables related to muscle force and stress were not included as they were not measured separately for different regions of the MG. To determine if the pMG and dMG occupied different regions of muscle function space, four-way ANOVAs were performed with speed (fixed), incline (fixed), muscle region (fixed) and individual (random) as the independent variables and the PC scores from a particular axis as the dependent variable.

To account for multiple observations within each individual, the *F*-values were calculated by dividing the main effect (e.g. speed) by the interaction term involving individual and the factor of interest (e.g. speed \times individual). Further details of this calculation can be found in (Zar, 1996). $P < 0.05$ was used as the criterion for statistical significance in all tests. SYSTAT version 9 (SPSS Inc., Chicago, IL, USA) was used for all statistical analyses. Unless stated otherwise, all values are means \pm s.e.m.

RESULTS

Morphology and general *in vivo* patterns

The mean mass and cross-sectional area of the MG is almost twice that of the LG (Table 1). However, both muscles have comparable mean pennation angles and mean fascicle lengths (Table 1). In addition, there is little difference in mean pennation angle and mean fascicle length between the pMG and dMG (Table 1).

The LG generally shortened throughout the stance phase of the stride despite changes in speed and incline (Fig. 2A and Fig. 3A). The pMG underwent a shorten–stretch–shorten cycle when the birds walked or ran on a level treadmill (Fig. 2A and Fig. 3A); however, this pattern was not apparent during inclined locomotion (Fig. 3A). Finally, the dMG remained relatively isometric regardless of speed or incline (Fig. 2A and Fig. 3A). While force generation in the LG and MG began at, or immediately after, footfall (Fig. 2B and Fig. 3B), the onset of force in the LG began, on average, 7.0 ± 1.6 ms before the onset of force in the MG.

EMG results

Mean EMG spike amplitude (MSA) increased significantly with an increase in speed for both muscles and regions within the MG regardless of incline (Fig. 4A) ($P < 0.05$, ANOVA). However, MSA was not affected by changes in incline ($P > 0.05$). Maximum muscle force and MSA were positively, and significantly, correlated for the LG ($r^2 = 0.52$, $P < 0.001$), pMG ($r^2 = 0.31$, $P < 0.001$) and dMG ($r^2 = 0.58$, $P < 0.001$) (Fig. 4B).

When walking at 0.5 m s^{-1} , the LG, pMG and dMG were activated slightly before the onset of muscle force (Fig. 5), which was almost coincident with footfall. The offset of EMG activity (relative to force duration), however, differed between the muscle regions such that the LG ($92.5 \pm 10.0\%$) and dMG ($81.9 \pm 5.3\%$) remained active longer than the pMG ($60.4 \pm 4.9\%$) (Fig. 5). When running at

Table 1. Morphological data for the muscles examined in this study

Muscle region	<i>N</i>	Mass (g)	Fascicle length (mm)	Pennation angle (degrees)	<i>PCSA</i> (mm ²)
LG	4	10.6 \pm 1.1	18.6 \pm 1.1	23.7 \pm 0.9	488.6 \pm 56.8
pMG*	4	18.9 \pm 2.1	17.8 \pm 0.7	28.0 \pm 1.5	910.7 \pm 120.8
dMG*	4	18.9 \pm 2.1	17.4 \pm 0.9	27.1 \pm 1.4	910.7 \pm 120.8

LG, lateral gastrocnemius; pMG, proximal region of the medial gastrocnemius; dMG, distal region of the medial gastrocnemius; *PCSA*, physiological cross-sectional area.

*Note that values for mass and *PCSA* are for the entire MG.

Values are means \pm s.e.m.

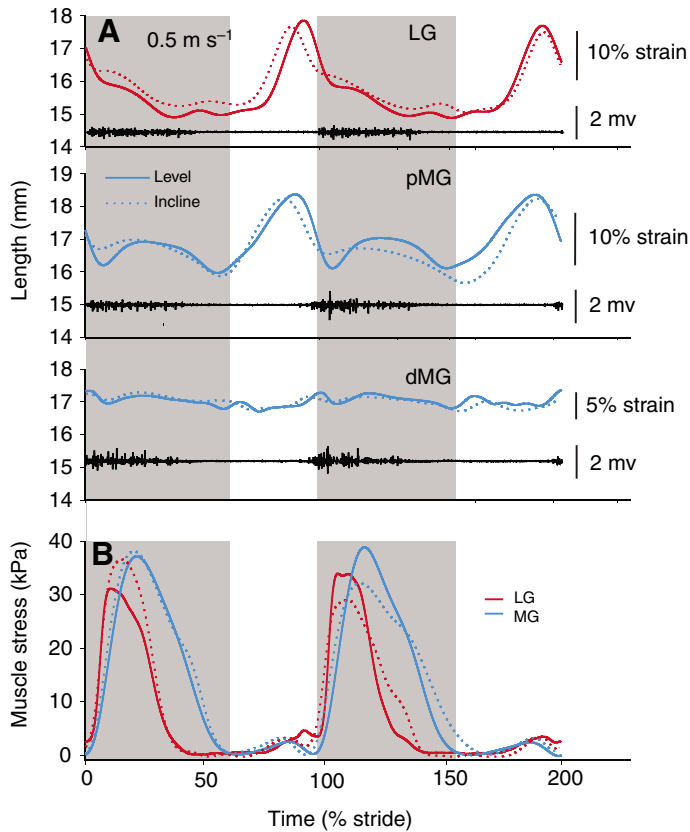


Fig. 2. Two consecutive representative strides at 0.5 m s^{-1} on a level (solid lines) and inclined (broken lines) treadmill showing the changes in fascicle length (A) for the LG (red), pMG (blue) and dMG (blue). A scale bar for fascicle strain is to the right of each panel. The corresponding EMG signals (for level only) are also shown in black with a scale bar to the right. The shaded regions indicate the stance phases of the strides. (B) Muscle stress corresponding with the strides in A for the LG (red) and MG (blue).

2.0 m s^{-1} , all muscle regions were activated earlier (compared with walking) relative to the onset of force (Fig. 5). Whereas the LG and pMG were deactivated earlier when running compared with walking, the dMG offset did not differ between walking and running, which led to an increase in EMG duration.

Fascicle strain and strain rate

On a level treadmill (when walking), the net shortening of the LG ($8.3 \pm 1.2\%$) and pMG ($8.5 \pm 1.8\%$) fascicles were similar; whereas the dMG remained relatively isometric ($1.9 \pm 0.5\%$ shortening) (Fig. 6). When the birds ran on a level treadmill, the net fascicle shortening was greater (compared with walking) for both the LG ($13.4 \pm 3.1\%$) and pMG ($14.8 \pm 2.9\%$). However, the effect of speed on fascicle strain during inclined locomotion was only apparent for the LG (shortening increased by 6.3%) (Fig. 6A). In fact, the pMG exhibited a 4.1% decrease in fascicle shortening with an increase in speed when moving on the inclined treadmill. The only effect of incline on fascicle strain was for the pMG during walking conditions (shortening increased by 8.1%). Fascicle strain in the dMG was not affected by incline or speed (Fig. 6A). During force production, the LG (overall mean, $-2.1 \pm 0.5 \text{ L s}^{-1}$) consistently exhibited a greater fascicle strain rate compared with the pMG (overall mean, $-1.4 \pm 0.2 \text{ L s}^{-1}$) and dMG

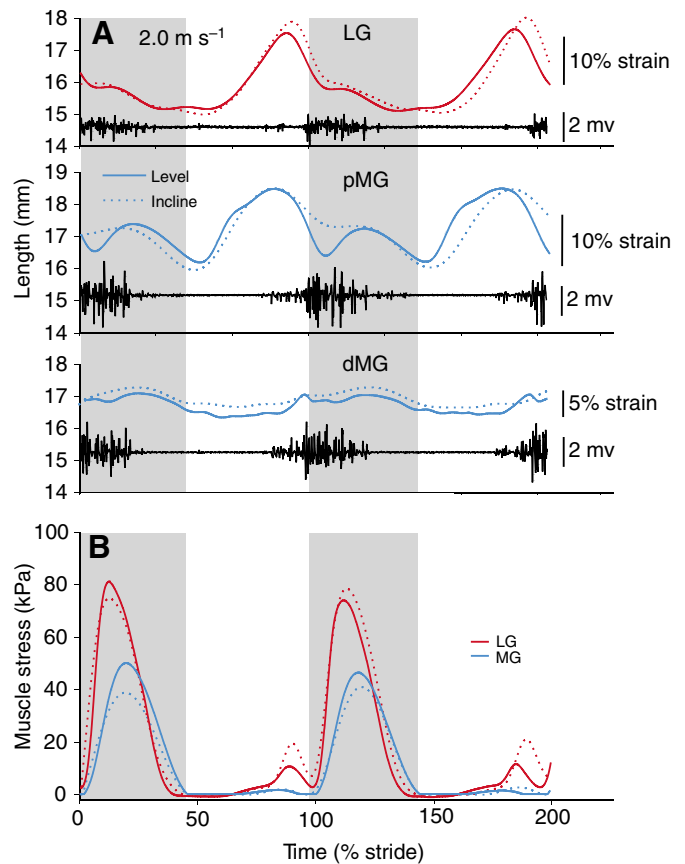


Fig. 3. Two consecutive representative strides at 2.0 m s^{-1} on a level (solid lines) and inclined (broken lines) treadmill showing the changes in fascicle length (A) for the LG (red), pMG (blue) and dMG (blue). A scale bar for fascicle strain is to the right of each panel. The corresponding EMG signals (for level only) are also shown in black with a scale bar to the right. The shaded regions indicate the stance phases of the strides. (B) Muscle stress corresponding with the strides in A for the LG (red) and MG (blue).

(overall mean, $-0.4 \pm 0.05 \text{ L s}^{-1}$) (Fig. 6B). In addition, the pMG exhibited a much higher strain rate than the dMG. Fascicle strain rate generally increased in all muscles and regions with an increase in locomotor speed ($P < 0.05$, ANOVA) (Fig. 6B) but was not significantly affected by incline.

Muscle force and stress

Muscle stress (and force) increased with speed on the level surface for both the MG (0.5 m s^{-1} , $28.9 \pm 2.2 \text{ kPa}$; 2.0 m s^{-1} , $40.7 \pm 3.2 \text{ kPa}$) and LG (0.5 m s^{-1} , $31.9 \pm 3.0 \text{ kPa}$; 2.0 m s^{-1} , $73.0 \pm 4.0 \text{ kPa}$), but this increase was more pronounced for the LG (Fig. 7). Whereas the MG generated more force than the LG when walking at 0.5 m s^{-1} (Fig. 8A), there was no significant difference in force generation when running at 2.0 m s^{-1} (Fig. 8A). Because PCSA of the MG was nearly double that of the LG (Table 1), this means that there was no significant difference in muscle stress when walking, but the LG generated significantly more stress than the MG when running (Fig. 7 and Fig. 8B). Incline did not affect force or stress in the LG and MG. Synergist force generation was dominated by the LG during the first half of stance but by the MG during the second half (Fig. 8C).

The ADS of the pMG was consistently lower than that of the dMG (Fig. 9). The greatest difference, however, occurred when the

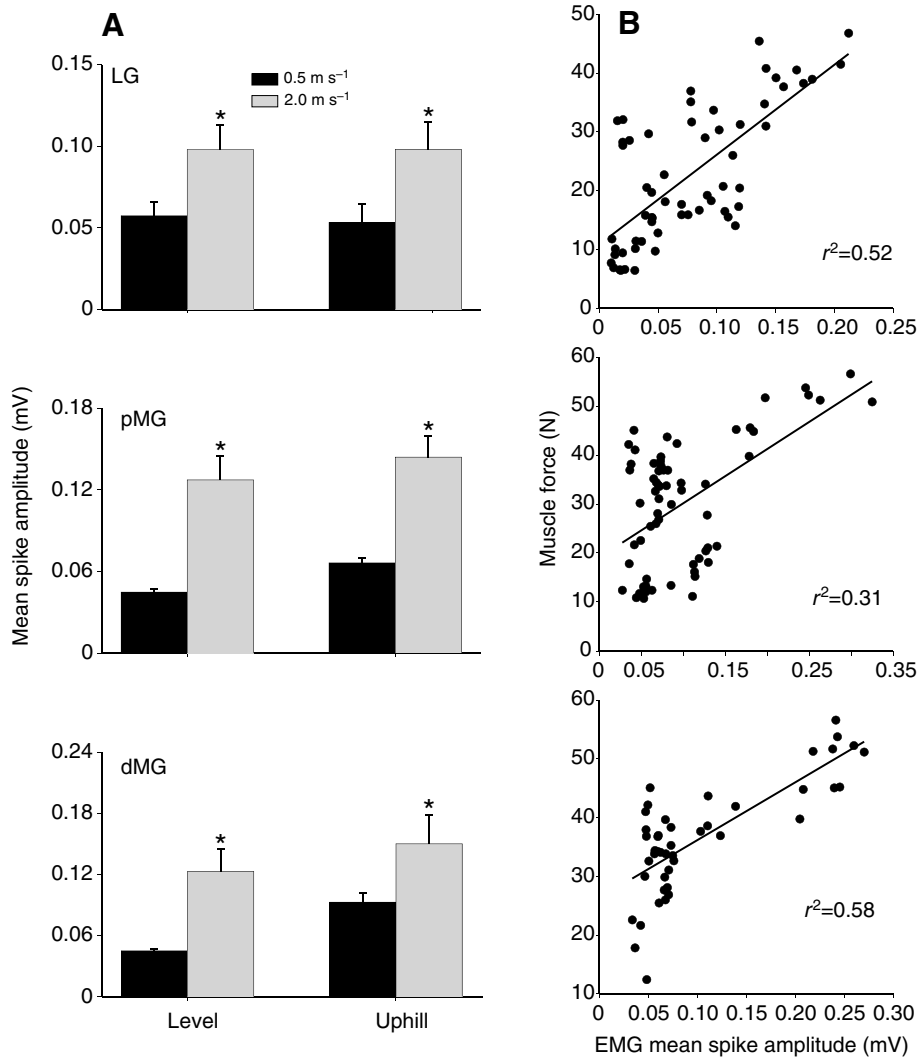


Fig. 4. (A) Mean EMG spike amplitude (MSA) for the LG (top), pMG (middle) and dMG (bottom). The black and grey bars represent strides at 0.5 and 2.0 m s⁻¹, respectively. Strides on the level surface are on the left of each panel and strides on the inclined surface are on the right. Asterisks indicate a significant effect of locomotor speed from an ANOVA ($P < 0.05$). Values are means \pm s.e.m. ($N = 4$). (B) Regressions of MSA versus maximum muscle force for the LG (top), pMG (middle) and dMG (bottom). Force and MSA were significantly, and positively, correlated for the LG ($r^2 = 0.52$, $P < 0.001$), pMG ($r^2 = 0.31$, $P < 0.001$) and dMG ($r^2 = 0.58$, $P < 0.001$). LG, $y = 152.9x + 10.8$; pMG, $y = 110.7x + 19.1$; dMG, $y = 98.3x + 26.3$.

birds were running on the level surface at 2.0 m s⁻¹ (dMG, 90.2 \pm 11.9 N mm⁻¹; pMG, 25.4 \pm 3.9 N mm⁻¹). The LG consistently exhibited a lower ADS compared with the pMG and dMG (Fig. 9).

Muscle work

The LG consistently performed net positive work at all speeds on level (0.5 m s⁻¹, 1.3 \pm 1.2 J kg⁻¹; 2.0 m s⁻¹, 5.0 \pm 1.1 J kg⁻¹) and inclined (0.5 m s⁻¹, 2.4 \pm 0.6 J kg⁻¹; 2.0 m s⁻¹, 8.3 \pm 2.0 J kg⁻¹) surfaces (Figs 10 and 11) and consistently performed more positive work than both the pMG and dMG (Fig. 11). The pMG, on the other hand, exhibited a considerable amount of negative work (compared with the LG) when the birds were walking on the level (-0.6 \pm 0.06 J kg⁻¹) but performed less negative (-0.3 \pm 0.04 J kg⁻¹) and more positive (1.7 \pm 0.3 J kg⁻¹ compared with 1.1 \pm 0.1 J kg⁻¹ on the level) work on an inclined surface (Figs 10 and 11). Across all conditions, the dMG performed little positive work (mean, 0.4 \pm 0.04 J kg⁻¹) (Figs 10 and 11).

On the level surface, positive muscle work increased significantly with an increase in speed for both the LG (increase of 3.6 J kg⁻¹; $P < 0.05$, ANOVA) and pMG (increase of 0.5 J kg⁻¹; $P < 0.05$, ANOVA) but not the dMG (Fig. 11). On an inclined surface, positive work increased with speed only for the LG (increase of 5.5 J kg⁻¹; $P < 0.05$, ANOVA) (Fig. 11). The amount of negative work

performed was not affected by incline or speed for any muscle or region.

Muscle function in multivariate space

The PCA revealed several interesting clusters of variables that loaded strongly with certain axes. For the LG, variables related to muscle force (and stress) loaded strongly on PC axis 1, variables related to fascicle strain loaded strongly on PC axis 2, and EMG variables loaded strongly on PC axis 3 (Table 2). Speed significantly affected PC axis 1 ($P < 0.05$, ANOVA) (Fig. 12), indicating that force and stress increased with speed, and EMG duration decreased. Speed did not affect any other PC axis for the LG, and incline did not affect any PC axis of either muscle. For the pMG, variables related to fascicle strain, force and stress, and EMG variables all loaded strongly on PC axis 1 (Table 3), although this axis was not affected by speed or incline. PC axis 3 was significantly affected by speed (Fig. 12) ($P < 0.05$, ANOVA), and force and EMG duration loaded strongly on this axis (Table 3).

The PCA addressing variables related to the pMG and dMG identified key variables that differed between the two muscle regions (Fig. 13). Muscle region significantly affected PC axis 1, and speed significantly affected PC axis 3. Variables related to fascicle strain loaded strongly on PC axis 1 (Table 4), indicating that these

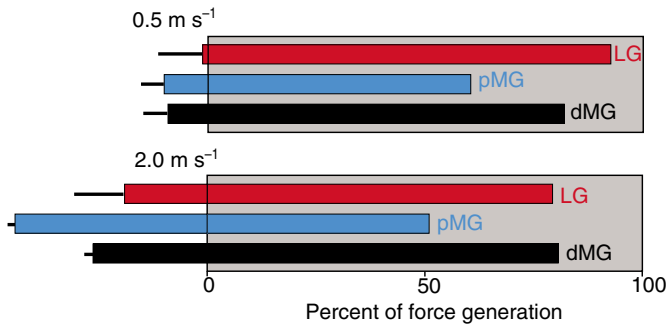


Fig. 5. The relative onset, offset and duration of the EMG bursts relative to force generation in the LG (red bars), pMG (blue bars) and dMG (black bars). Note that the onset of force is almost coincident with footfall for both the LG and MG. The upper and lower panels represent speeds of 0.5 and 2.0 m s⁻¹, respectively. Values are means \pm s.e.m. ($N=4$) of the EMG burst duration. Note that for all three muscle regions, the onset of EMG activity precedes the onset of force generation to a greater extent when running at 2.0 m s⁻¹ compared with walking at 0.5 m s⁻¹. There were no effects of incline (not shown).

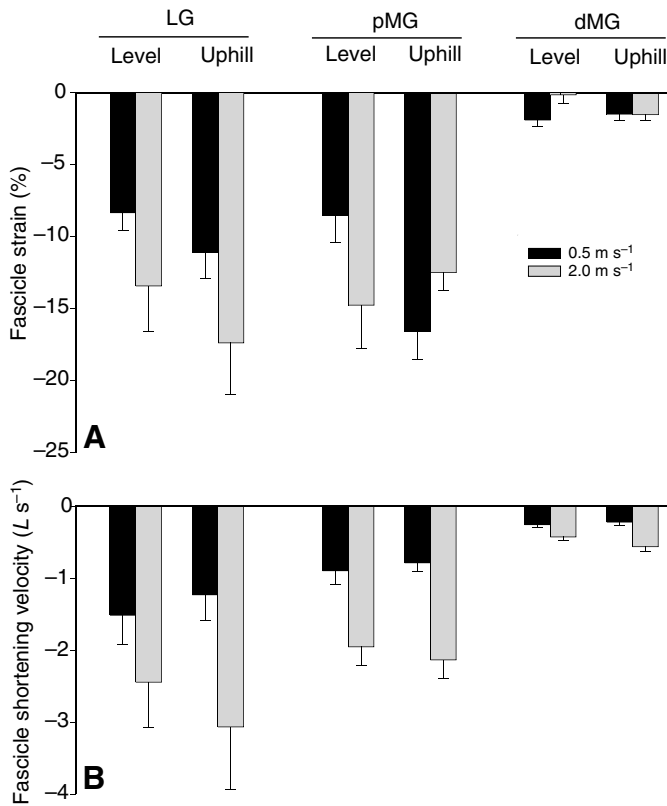


Fig. 6. Mean fascicle strain (A) and fascicle shortening velocity (B) for the LG, pMG and dMG walking (black; 0.5 m s⁻¹) and running (grey; 2.0 m s⁻¹) on a level (left pair of bars) and inclined (right pair of bars) treadmill. Note that strain increased for the LG and pMG with an increase in running speed on the level treadmill, but only for the LG on an inclined treadmill. Values are means \pm s.e.m. ($N=4$).

variables significantly differed between the two regions of the muscle. EMG duration loaded strongly on PC axis 3 (Table 4). In general, the pMG exhibited greater variation on PC axis 1 compared with the dMG.

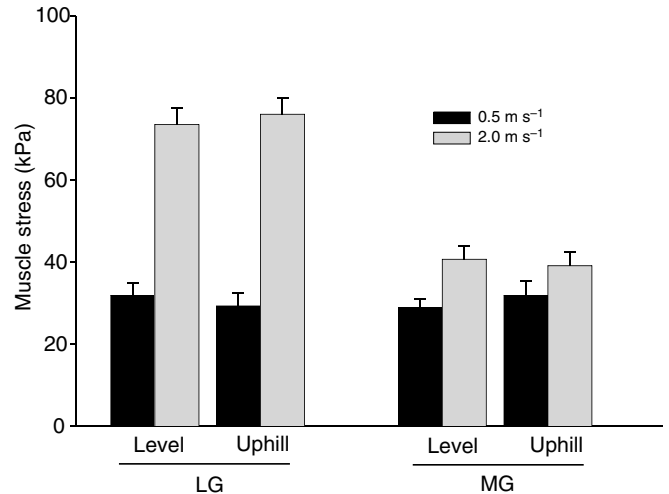


Fig. 7. Mean peak muscle stress for the LG and MG walking (black; 0.5 m s⁻¹) and running (grey; 2.0 m s⁻¹) on a level (left pair of bars) and inclined (right pair of bars) treadmill. Note that muscle force and stress increased with running speed on the level and inclined treadmill for both muscles, but force and stress were not affected by incline. Values are means \pm s.e.m. ($N=4$).

DISCUSSION

We found substantial heterogeneity between the two hindlimb muscle synergists studied here and between the proximal and distal region of a single muscle of guinea fowl under dynamic locomotor conditions. The LG consistently performed more positive work than its synergist, the MG, and this difference increased markedly with a change in gait and an increase in speed. Further, based on measured differences in fascicle strain, the pMG performed considerably more positive work than the dMG, highlighting the functional diversity that can occur within a single muscle. Although speed and incline both alter the mechanical demands placed on the locomotor system, speed influences the distal muscles of guinea fowl to a much greater extent than incline.

Effects of speed and incline

Changes in locomotor speed have considerable impacts on terrestrial vertebrate energetics (Taylor et al., 1982; Chappell et al., 2004), limb kinematics (Gatesy, 1999; Irschick and Jayne, 1999; Jayne and Irschick, 1999; Hutchinson et al., 2006), muscle activation patterns (Hoyt et al., 2005; Higham et al., 2008), muscle strain (Nelson and Jayne, 2001; Roberts et al., 2007; Higham et al., 2008) and muscle force (Walmsley et al., 1978; Daley and Biewener, 2003; Kaya et al., 2003; Higham et al., 2008). These changes are associated with the increased energy requirements that accompany an increase in running speed. In addition to a decrease in duty factor and limb support time, which require greater weight-related forces, the kinetic energy changes involved in moving the limbs of guinea fowl increase as the 1.75 power of speed (Fedak et al., 1982). The LG and MG exhibited a substantial increase in muscle force with an increase in locomotor speed, and this is a result of increased motor activation (i.e. increased mean spike amplitude of the EMG signals) (Fig. 4). With increasing speed, guinea fowl exhibited an increase in stride frequency and stride length, which resulted, in part, from an increase in knee flexion during stance (Gatesy, 1999). The increased knee flexion is likely associated with the increased LG (knee flexor) shortening that occurred with an increase in speed in

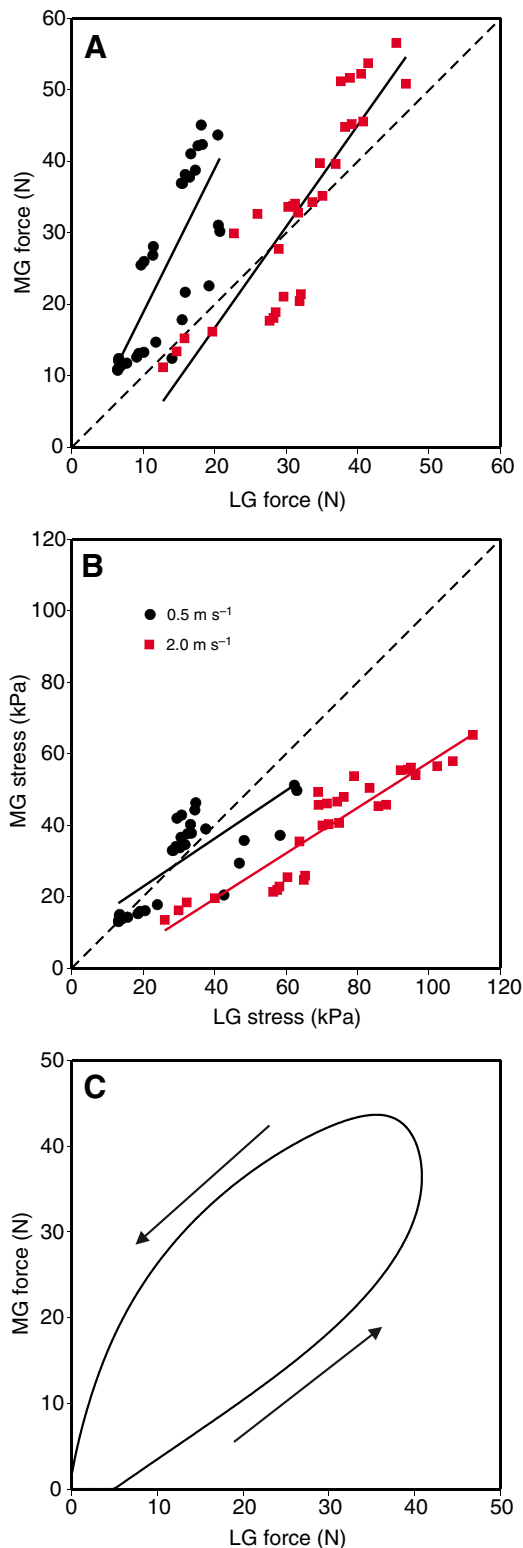


Fig. 8. Peak LG force *versus* peak MG force (A) and peak LG stress *versus* peak MG stress (B) during walking (black circles) and running (red triangles). The broken line represents the null hypothesis that both muscles share force and stress equally. Note that, while the MG generates more force relative to the LG, the LG consistently generates more stress. As speed increases, the LG exhibits a greater increase in force and stress compared with the MG. Also shown is LG force plotted against MG force (C) for a representative sequence of a bird running at 2 m s⁻¹ on an inclined treadmill. The arrows indicate the direction of the loop starting at the onset of force in the LG. Note that force generation is weighted towards the LG during the early stages of stance and then towards the MG during the later part of stance. This pattern is extremely consistent among and between animals.

wallabies exhibit only a slight increase in positive work with an increase in speed (Biewener et al., 1998). Similarly, a prior study of guinea fowl (Daley and Biewener, 2003) found no increase in work performed by the digital flexor-IV muscle with increased speed (0.7–2.0 m s⁻¹). This suggests that the increased work necessary to hop or run with increased stride length comes from proximal hindlimb muscles. However, Daley and Biewener observed a 2.5-fold increase in net work with an increase in speed for the LG, and we observed a 3.9-fold increase (Fig. 11). While proximal muscles may contribute to the increased work associated with running faster in guinea fowl, it is clear that distal muscles also contribute to the increase in work with an increase in speed. This notion is corroborated by recent work examining blood flow to various limb muscles of guinea fowl during running (Ellerby et al., 2005), in which a 3.8-fold increase in blood flow to the LG was observed when animals increased speed from a walk (0.5 m s⁻¹) to a medium run (1.5 m s⁻¹). This suggests that the increase in blood flow during aerobic running is linked to the increased work that the muscle must perform at higher speeds.

As noted above, Daley and Biewener (Daley and Biewener, 2003) obtained higher values of mass-specific LG work than in our study, which can be attributed to methodological differences between the studies. First, the guinea fowl in our study are almost twice the mass

the current study. Ultimately, the LG, and to a lesser extent the MG, increased its mechanical work output with an increase in running speed, highlighting a key functional role of these distal muscles.

Muscles that recover a large amount of energy from storage in tendons may show little change in muscle work with increases in running or hopping speed. For example, the LG and plantaris of

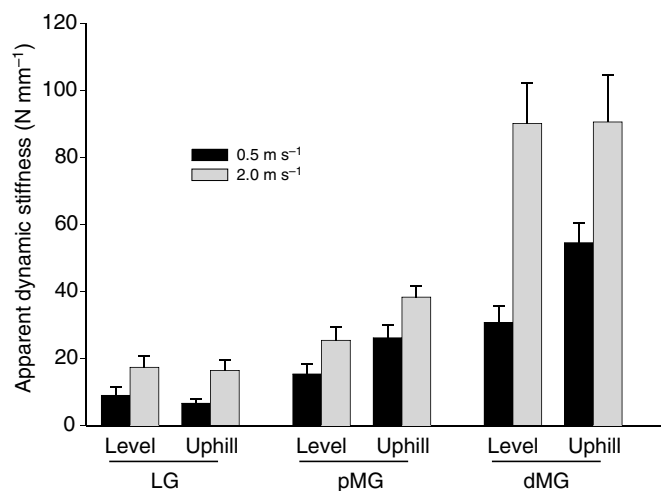


Fig. 9. Apparent dynamic stiffness (ADS) for the LG, pMG and dMG during walking (black; 0.5 m s⁻¹) and running (grey; 2.0 m s⁻¹) on a level (left pair of bars) and inclined (right pair of bars) treadmill. Note that the dMG exhibited a much higher ADS compared with the pMG and LG. See Materials and methods regarding the calculation of ADS. Values are means ± s.e.m. (N=4).

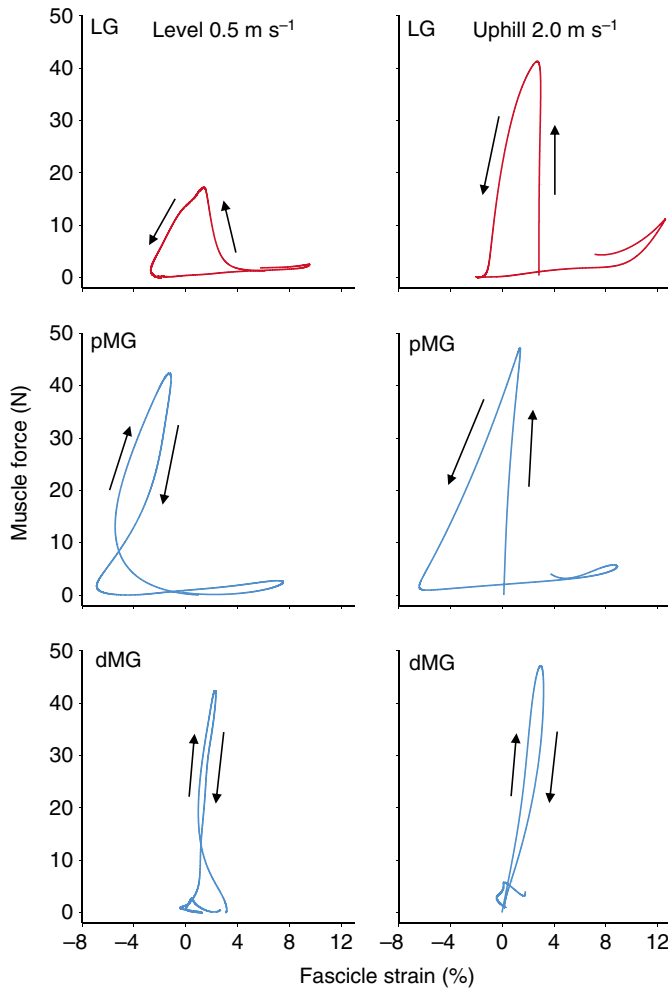


Fig. 10. Representative *in vivo* work loops for the LG (red; upper panels), pMG (blue; middle panels) and dMG (blue; bottom panels) walking at 0.5 m s^{-1} on a level treadmill (left column) and running at 2.0 m s^{-1} on an inclined treadmill (right column). The area within each loop represents the net work done by each muscle and muscle region. Arrows indicate the direction of the work loop, such that a counter-clockwise loop indicates net positive work and a clockwise loop indicates net negative work (energy absorption). Note that the amount of positive work increased substantially with an increase in speed and incline for the LG.

of the birds used by Daley and Biewener. Despite this, the measured LG force in our study was almost identical to that estimated by Daley and Biewener, leading to lower values of mass-specific work in our study. Second, Daley and Biewener quantified LG work by measuring strain in the LG but force from the common tendon of the LG and MG. Thus, equal stress between these synergists was assumed, which is problematic based on the results of our study. Finally, the timing of force generation by the LG and MG differ (Fig. 2), something that Daley and Biewener could not observe given that force was measured from the common tendon (Daley and Biewener, 2003). When walking, the MG generates force for approximately 100ms after the LG has stopped generating force (Fig. 2), suggesting that work performed by the LG would be overestimated if forces from the LG and MG were measured together. The values of muscle work in the current study are considerably lower than those reported by Higham et al. for the LG

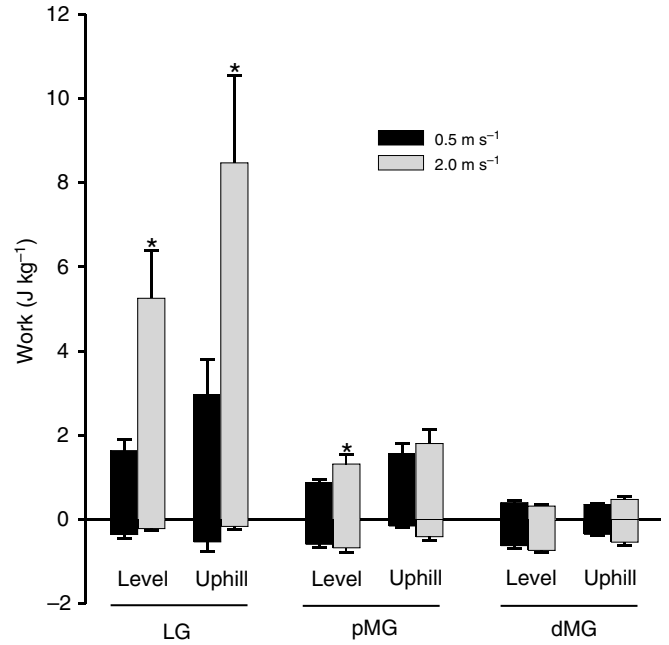


Fig. 11. Mean positive and negative work per stride performed by the LG, pMG and dMG walking (black; 0.5 m s^{-1}) and running (grey; 2.0 m s^{-1}) on a level (left pair of bars) and inclined (right pair of bars) treadmill. Note that the positive work performed by the LG consistently exceeded that of both the pMG and dMG. Asterisks indicate a significant effect of speed from an ANOVA ($P < 0.05$). Values are means \pm s.e.m. ($N=4$).

Table 2. Loadings from a principal components analysis, including 13 variables related to LG muscle function

Variable	PC1	PC2	PC3
Strain _{force onset to force max}	-0.12	-0.94	0.21
Strain _{force max to force offset}	-0.37	0.50	0.40
Strain _{swing}	0.39	0.79	-0.35
Strain _{net}	-0.37	-0.73	0.49
Force _{max}	0.93	0.04	0.32
Force _{mean}	0.87	-0.18	0.37
Force _{duration}	-0.73	0.47	0.33
Stress _{max}	0.88	0.42	0.06
Stress _{mean}	0.94	0.16	0.15
EMG _{duration}	-0.66	0.59	0.35
EMG _{onset relative to force onset}	0.39	-0.54	-0.06
MSA	0.59	0.16	0.60
RIA	-0.27	0.23	0.65

PC1, PC2 and PC3 explained 40.4, 26.7 and 14.3% of the total variance, respectively.

LG, lateral gastrocnemius; EMG, electromyogram; MSA, mean spike amplitude of the EMG burst; RIA, rectified integrated area of the EMG burst.

Loadings >0.6 are in bold.

and MG of guinea fowl (Higham et al., 2008). This can also be attributed to methodological differences. Higham et al. multiplied regional changes in fascicle strain by the difference in muscle and fascicle lengths (the muscles were approximately seven times longer than the fascicles), which was an overestimate of whole muscle work.

Studies of locomotor muscle function typically involve the quantification of numerous variables related to activation, strain and

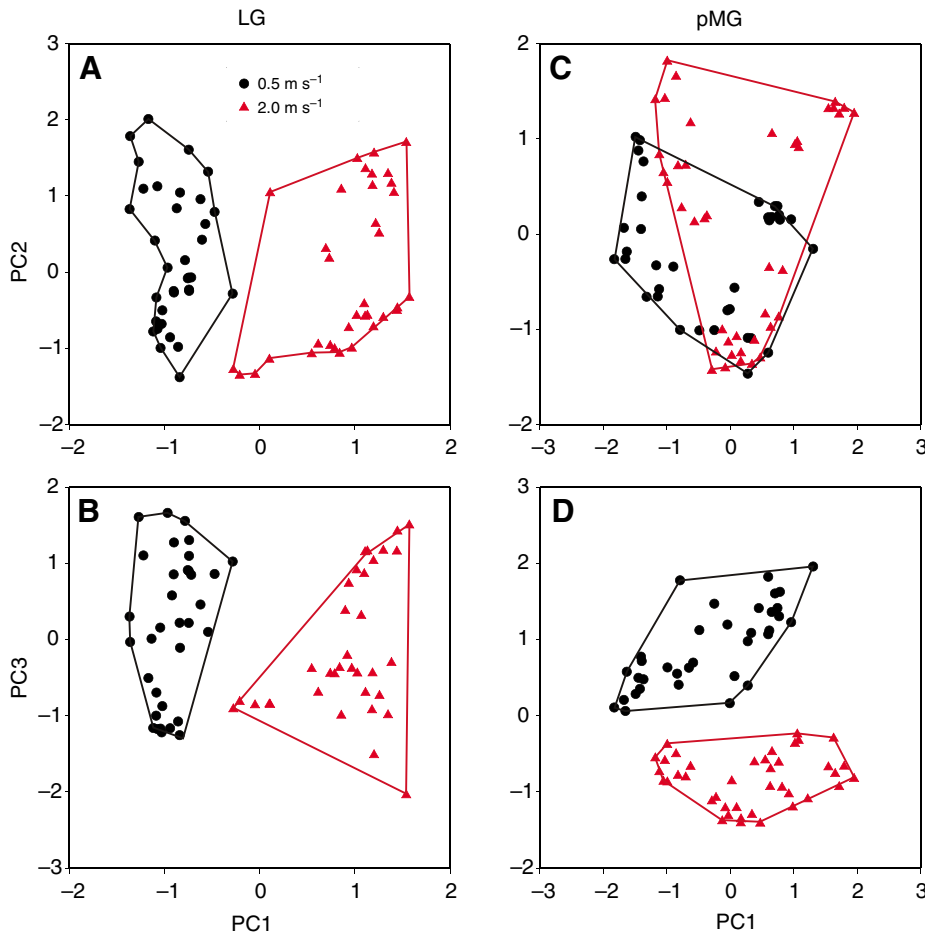


Fig. 12. Results (factor scores) from principal components analyses (PCA) using 13 variables related to muscle function for the LG (A,B) and pMG (C,D) during walking (black circles) and running (red triangles). The top panels (A,C) show PC1 versus PC2, and the bottom panels (B,D) show PC1 versus PC3. Note that PC1 separated the two speeds for the LG, and PC3 separated the two speeds for the pMG. See Tables 2 and 3 for component loadings. For the LG, variables related to stress and force loaded strongly on PC1 whereas variables related to force and EMG duration loaded strongly on PC3 for the pMG.

Table 3. Loadings from a principal components analysis including 13 variables related to pMG muscle function

Variable	PC1	PC2	PC3
Strain _{force onset to force max}	-0.08	0.94	0.23
Strain _{force max to force offset}	0.60	-0.14	0.17
Strain _{swing}	-0.80	-0.23	-0.37
Strain _{net}	0.23	0.86	0.31
Force _{max}	0.95	0.02	-0.13
Force _{mean}	0.97	0.01	0.05
Force _{duration}	-0.01	-0.30	0.93
Stress _{max}	0.70	-0.57	-0.38
Stress _{mean}	0.75	-0.54	-0.16
EMG _{duration}	0.14	-0.19	0.91
EMG _{onset relative to force onset}	0.00	0.66	-0.37
MSA	0.56	0.54	-0.45
RIA	0.67	0.40	0.23

PC1, PC2 and PC3 explained 36.4, 25.5 and 19.9% of the total variance, respectively.

pMG, proximal region of the medial gastrocnemius; EMG, electromyogram; MSA, mean spike amplitude of the EMG burst; RIA, rectified integrated area of the EMG burst.

Loadings >0.6 are in bold.

Table 4. Loadings from a principal components analysis, including eight variables related to within MG muscle function

Variable	PC1	PC2	PC3
Strain _{force onset to force max}	0.73	0.15	0.03
Strain _{force max to force offset}	0.65	-0.47	-0.35
Strain _{swing}	-0.86	0.38	0.18
Strain _{net}	0.92	-0.11	-0.16
EMG _{duration}	0.18	-0.63	0.74
EMG _{onset relative to force onset}	0.30	0.69	0.23
MSA	0.51	0.73	-0.12
RIA	0.66	0.24	0.56

PC1, PC2 and PC3 explained 41.8, 23.4 and 13.9% of the total variance, respectively.

MG, medial gastrocnemius; EMG, electromyogram; MSA, mean spike amplitude of the EMG burst; RIA, rectified integrated area of the EMG burst.

Loadings >0.6 are in bold.

force. This inflates the probability of incorrectly rejecting the null hypothesis (increasing type-I error rate and decreasing statistical power), requiring an adjustment for multiple tests of significance using, for example, the sequential Bonferroni method (Rice, 1989). Using a PCA limits this problem by reducing the dimensionality of

a large dataset and provides a mechanism for identifying the key variables that are influenced by various ecological factors (e.g. speed and/or incline). In our dataset, the variables related to force (and stress) magnitude and duration were primarily influenced by locomotor speed. In addition, we found that the axis explaining the most variation in LG function (PC1) separates the two locomotor speeds. Thus, a substantial amount of variation in LG function (40.4%) can be explained by changes in locomotor speed. By contrast, PC1 for the pMG data does not distinguish between

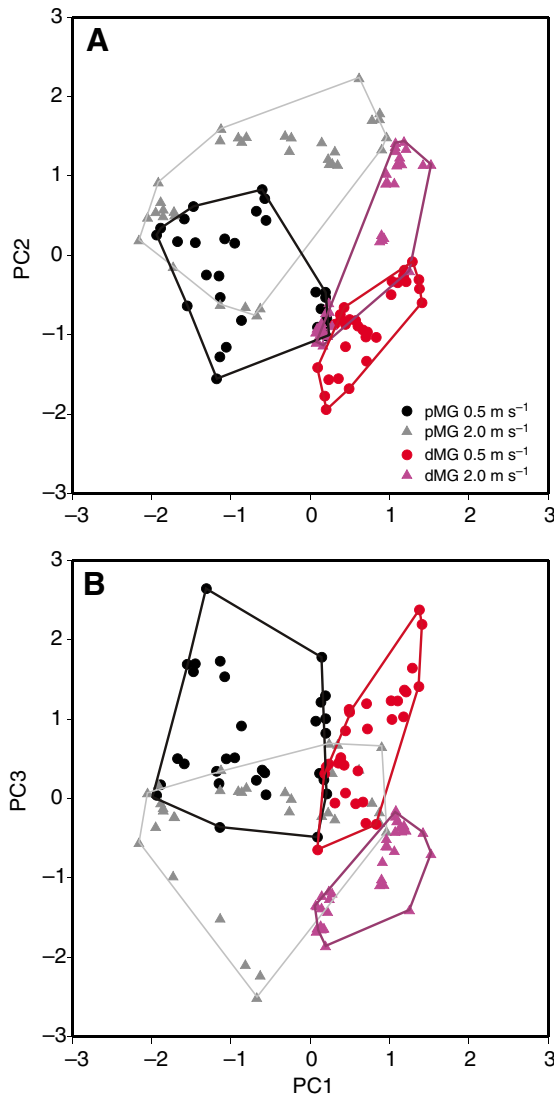


Fig. 13. Results (factor scores) from principal components analyses (PCA) using eight variables related to muscle function for the pMG during walking (black circles) and running (grey triangles), and for the dMG during walking (red circles) and running (pink triangles). (A) PC1 versus PC2. (B) PC1 versus PC3. Note that PC1 separated the two regions of the muscles, and PC3 separated the two speeds. See Table 4 for component loadings.

locomotor speeds, suggesting that the effects of locomotor speed on pMG function are not as pronounced.

Inclines affect overall limb movements of terrestrial vertebrates (Carlson-Kuhta et al., 1998; Higham and Jayne, 2004b; Lammers et al., 2006), which can cause changes in muscle activation, strain and force production (Roberts et al., 1997; Daley and Biewener, 2003; Gabaldon et al., 2004; Higham and Jayne, 2004a; Roberts et al., 2007). We also observed changes in muscle contractile behavior with changes in incline in the present study. During level running, the guinea fowl pMG exhibited a stretch before shortening during stance (Figs 2 and 3), likely increasing its force generation (Katz, 1939; Abbott and Aubert, 1952; Rassier et al., 2003). Because the MG primarily exerts an extensor moment at the knee (Higham et al., 2008), the muscle's initial stretch was

likely due to initial knee flexion that occurs immediately following footfall in guinea fowl (Gatesy, 1999). Interestingly, a pre-stretch of the pMG did not occur on the incline conditions, and initial knee flexion after footfall is typically absent during inclined locomotion in other bipedal birds (Higham and Nelson, in press) and mammals (Carlson-Kuhta et al., 1998). This suggests that the change in knee kinematics (Higham and Nelson, in press) is likely responsible for the lack of initial MG lengthening that we observed in guinea fowl during uphill locomotion (Figs 2 and 3). The lack of a pre-stretch of the pMG on the inclined surface also likely lowered the force-generating capabilities of this region of the muscle. This is supported by the fact that EMG MSA increased from level to incline at 2 m s^{-1} (Fig. 4A), but muscle force decreased (Fig. 7A). This speed also represents the most dramatic change in strain patterns recorded in the pMG (Fig. 3). By contrast, changes in incline did not influence the strain patterns of the dMG, highlighting the decoupling of function that can occur within a single muscle.

Stresses in the LG and MG of guinea fowl changed little with incline, similar to patterns of stress recorded in the LG of turkeys (Roberts et al., 1997) and the gastrocnemius and plantaris of wallabies (Biewener et al., 2004). However, in an earlier study, Daley and Biewener observed increases in the peak stresses acting in the LG (37%) and DF-IV (21%) when guinea fowl ran on a 16° incline versus on a level (Daley and Biewener, 2003). The basis for this difference is unclear but could reflect individual variation associated with the animals used in the two studies. Given the moderate increase in work by the LG and MG, proximal knee and hip extensors of guinea fowl are likely responsible for most of the increase in limb work during incline running, as is the case with wallabies (McGowan et al., 2007). Future work examining the roles of proximal and distal hindlimb muscles in relation to changes in contractile performance and work production is clearly needed but is also challenged by the difficulty of assessing work in proximal muscles, which must otherwise be inferred from patterns of joint work.

Heterogeneity between muscle synergists

The idea that muscle synergists can function dissimilarly has interested researchers for some time. For example, the cat MG exhibits an increase in force output as locomotor speed increases whereas the soleus (its synergist) exhibits a relatively constant force output with an increase in speed (Walmsley et al., 1978; Hodgson, 1983; Kaya et al., 2003). This shift in synergist function likely reflects differences in the muscles' motor unit composition (Hodgson, 1983): the soleus being comprised of slow-twitch fibers and the MG of a mixture of fast and slow-twitch fibers. Although the guinea fowl LG and MG (synergists at the ankle) are more similar to each other with respect to fiber type composition than are the cat soleus and MG (J. W. Hermanson, T.E.H. and A.A.B., unpublished), they also differ considerably in the overall pattern of force, strain and work. For example, force and work in the LG increased to a much greater extent with an increase in locomotor speed compared with the MG. This supports the idea that factors other than fiber composition, such as recruitment, contraction kinetics, anatomy, history-dependent effects and contraction velocities, can contribute to the functional differences observed between muscle synergists.

We also found that the operating stress of the MG was less than that of the LG during running, suggesting that the MG has a greater reserve capacity for other motor tasks. For example, it has been suggested that muscles operating with the greatest reserve capacity

are likely the most important power producers during acceleration or jumping (Roberts, 2001). In a variety of vertebrates, accelerating and jumping requires a large amount of muscle power (Aerts, 1998; Roberts and Marsh, 2003; Henry et al., 2005; McGowan et al., 2005) relative to steady locomotion. In addition, direct measurements of stresses from ankle extensors during jumping and acceleration reveal that they can far exceed those of steady locomotion (Biewener et al., 1988). Future work examining how LG and MG forces vary across different locomotor behaviors (e.g. jumping and turning), combined with *in vivo* measurements of muscle contractile properties, are needed to examine more fully how recruitment of these muscle synergists is varied with respect to their functional roles.

Functional heterogeneity within a single muscle

We found considerable functional differences between the proximal and distal regions of the MG, such that the pMG performed significantly more positive and net work than the dMG across all conditions. This was associated with a substantial difference in the ADS of the distal *versus* the proximal region of the MG (Fig. 9). This difference in ADS is likely due to the extensive aponeurosis into which the dMG fascicles insert. Because aponeurotic connective tissue is less compliant than passive muscle (Ettema and Huijing, 1989; Van Bavel et al., 1996), it has been thought to contribute to fascicle strain heterogeneity in other muscles. For example, based on cine-phase magnetic resonance imaging (MRI), the distal region of the human biceps brachii was observed to undergo 3.7% shortening during a 15% maximum voluntary contraction, whereas the mid-portion of the muscle shortened 28.2% (Pappas et al., 2002). This strain heterogeneity likely resulted from an extensive internal longitudinal aponeurosis that spans the distal third of the muscle, limiting fiber shortening in this region. Given that aponeurotic tissue is fairly common, a key question is whether there is a benefit to limiting the amount of fascicle shortening. Elegant studies have shown that an increase in fascicle shortening velocity will result in decreased force production (Hill, 1938). Thus, contracting isometrically due to the aponeurosis, as is the case for the dMG of guinea fowl, allows the muscle region to generate force economically (Roberts et al., 1997). The lower strain and shortening velocities of the dMG (relative to the pMG) (Fig. 6) will ultimately allow more effective force transmission and enhance the ability of the distal region to resist tensile forces.

Given the architectural complexity that exists within many muscles (Herring et al., 1979; Brown et al., 2003; Finni et al., 2003), non-uniform shortening as a result of muscle–aponeurosis architecture is likely of broader significance. In studies of the frog semimembranosus, Ahn et al. found that in-series fascicle strain heterogeneity occurred in association with the muscle's distal aponeurosis, causing the distal region to lengthen or strain little during shortening of the central and proximal regions of the muscle (Ahn et al., 2003). The presence of aponeurotic tissue may also limit the amount of variation that a region of muscle exhibits. We found that the dMG exhibited less variation along the primary axis of variation in the PCA (Fig. 13), suggesting that this region is more constrained than the pMG. In addition to aponeurotic tissue, fiber type differences within a muscle likely contribute to non-uniform shortening. For example, Higham et al. found that, in guinea fowl, the proximal region of the MG recruited faster motor units than the distal region (Higham et al., 2008). This likely contributed to the decreased strain in the distal region of the MG, given that slower motor units generate less

force than faster motor units (Kanda and Hashizume, 1992). Further work is necessary to understand the functional role of fiber type heterogeneity.

It is common to assume whole-muscle function by measuring function (e.g. EMG activity) at a single location (Higham and Jayne, 2004a). It is also common for musculoskeletal models to assume uniform strain within a muscle (Zajac, 1989). However, there is growing evidence, including the results from our study, that suggests that the assumption of functional homogeneity within a muscle should be approached with caution. If we estimated muscle work using only the fascicle strain data from the pMG, whole-muscle work would have been greatly over-estimated, given that the dMG performed up to 4.4 times less work than the pMG (Fig. 11). Future work addressing whether functional heterogeneity within a single muscle is pervasive among morphologically different muscles, and in the same muscles of different vertebrates, will provide needed insight into the complexity of muscle function. It will also be important to tease apart the contributions of various mechanisms that may underlie contractile heterogeneity in order to better predict the behavior of muscles under *in vivo* conditions.

LIST OF SYMBOLS AND ABBREVIATIONS

ADS	apparent dynamic stiffness
dMG	distal region of the medial gastrocnemius
EMG	electromyogram
L_f	fascicle length
LG	lateral gastrocnemius
L_o	resting length
L_{seg}	segment length
MG	medial gastrocnemius
MSA	mean spike amplitude
PCA	principal components analysis
PCSA	physiological cross-sectional area
pMG	proximal region of the medial gastrocnemius

We thank Craig McGowan for help with writing Matlab code and Pedro Ramirez for help with training and animal care. This work was supported by an NIH grant to A.A.B. (R01-AR047679).

REFERENCES

- Abbott, B. C. and Aubert, X. M. (1952). The force exerted by active striated muscle during and after change of length. *J. Physiol.* **117**, 77–86.
- Aerts, P. (1998). Vertical jumping in *Galago senegalensis*: the quest for an obligate mechanical power amplifier. *Philos. Trans. R. Soc. Lond. B Biol. Sci.* **353**, 1607–1620.
- Ahn, A. N. and Full, R. J. (2002). A motor and a brake: two leg extensor muscles acting at the same joint manage energy differently in a running insect. *J. Exp. Biol.* **205**, 379–389.
- Ahn, A. N., Monti, R. J. and Biewener, A. A. (2003). *In vivo* and *in vitro* heterogeneity of segment length changes in the semimembranosus muscle of the toad. *J. Physiol.* **549**, 877–888.
- Alexander, R. M. (1992). The work that muscles can do. *Nature* **357**, 360–361.
- Biewener, A. A. (1998). Muscle function *in vivo*: a comparison of muscles used for elastic energy savings *versus* muscles used to generate mechanical power. *Am. Zool.* **38**, 703–717.
- Biewener, A. A. (2003). *Animal Locomotion*. Oxford: Oxford University Press.
- Biewener, A. A. and Corning, W. R. (2001). Dynamics of mallard (*Anas platyrhynchos*) gastrocnemius function during swimming versus terrestrial locomotion. *J. Exp. Biol.* **204**, 1745–1756.
- Biewener, A. A., Blickhan, R., Perry, A. K., Heglund, N. C. and Taylor, C. R. (1988). Muscle forces during locomotion in kangaroo rats: force platform and tendon buckle measurements compared. *J. Exp. Biol.* **137**, 191–205.
- Biewener, A. A., Konieczynski, D. D. and Baudinette, R. V. (1998). *In vivo* muscle force-length behavior during steady-speed hopping in tammar wallabies. *J. Exp. Biol.* **201**, 1681–1694.
- Biewener, A. A., McGowan, C. P., Card, G. M. and Baudinette, R. V. (2004). Dynamics of leg muscle function in tammar wallabies (*M. eugenii*) during level *versus* incline hopping. *J. Exp. Biol.* **207**, 211–223.
- Blemker, S. S., Asakawa, D. S., Gold, G. E. and Delp, S. L. (2007). Image-based musculoskeletal modeling: applications, advances, and future opportunities. *J. Magn. Reson. Imaging* **25**, 441–451.
- Brown, N. A. T., Eawcak, C. E., McIlwraith, C. W. and Pandy, M. G. (2003). Architectural properties of distal forelimb muscles in horses, *Equus caballus*. *J. Morphol.* **258**, 106–114.

- Carlson-Kuhta, P., Trank, T. V. and Smith, J. L. (1998). Forms of forward quadrupedal locomotion. II. A comparison of posture, hindlimb kinematics, and motor patterns for upslope and level walking. *J. Neurophysiol.* **79**, 1687-1701.
- Carrasco, D. I., Lawrence, J. and English, A. W. (1999). Neuromuscular compartments of cat lateral gastrocnemius produce different torques about the ankle joint. *Motor Control* **3**, 436-446.
- Chanaud, C. M. and Macpherson, J. M. (1991). Functionally complex muscles of the cat hindlimb. III. Differential activation within biceps femoris during postural perturbations. *Exp. Brain Res.* **85**, 271-280.
- Chanaud, C. M., Pratt, C. A. and Loeb, G. E. (1991). Functionally complex muscles of the cat hindlimb. V. The roles of histochemical fiber-type regionalization and mechanical heterogeneity in differential muscle activation. *Exp. Brain Res.* **85**, 300-313.
- Chappell, M. A., Garland, T., Jr, Rezende, E. L. and Gomes, F. R. (2004). Voluntary running in deer mice: speed, distance, energy costs and temperature effects. *J. Exp. Biol.* **207**, 3839-3854.
- Daley, M. A. and Biewener, A. A. (2003). Muscle force-length dynamics during level versus incline locomotion: a comparison of *in vivo* performance of two guinea fowl ankle extensors. *J. Exp. Biol.* **206**, 2941-2958.
- Ellerby, D. J. and Marsh, R. L. (2006). The energetic costs of trunk and distal-limb loading during walking and running in guinea fowl *Numida meleagris*. II. Muscle energy use as indicated by blood flow. *J. Exp. Biol.* **209**, 2064-2075.
- Ellerby, D. J., Henry, H. T., Carr, J. A., Buchanan, C. I. and Marsh, R. L. (2005). Blood flow in guinea fowl *Numida meleagris* as an indicator of energy expenditure by individual muscles during walking and running. *J. Physiol.* **564**, 631-648.
- English, A. W. (1984). An electromyographic analysis of compartments in cat lateral gastrocnemius muscle during unrestrained locomotion. *J. Neurophysiol.* **52**, 114-125.
- Ettema, G. J. and Huijting, P. A. (1989). Properties of the tendinous structures and series elastic component of EDL muscle-tendon complex of the rat. *J. Biomech.* **22**, 1209-1215.
- Fedak, M. A., Heglund, N. C. and Taylor, C. R. (1982). Energetics and mechanics of terrestrial locomotion. II. Kinetic energy changes of the limbs and body as a function of speed and body size in birds and mammals. *J. Exp. Biol.* **79**, 23-40.
- Finni, T., Hodgson, J. A., Lai, A. M., Edgerton, V. R. and Sinha, S. (2003). Mapping of movement in the isometrically contracting human soleus muscle reveals details of its structural and functional complexity. *J. Appl. Physiol.* **95**, 2128-2133.
- Gabaldon, A. M., Nelson, F. E. and Roberts, T. J. (2004). Mechanical function of two ankle extensors in wild turkeys: shifts from energy production to energy absorption during incline versus decline running. *J. Exp. Biol.* **207**, 2277-2288.
- Gatesy, S. M. (1999). Guineafowl hind limb function. I. Cineradiographic analysis and speed effects. *J. Morphol.* **240**, 115-125.
- Gatesy, S. M. and Biewener, A. A. (1991). Bipedal locomotion: effects of speed, size and limb posture in birds and humans. *J. Zool. Lond.* **224**, 127-147.
- Gillis, G. B., Flynn, J. P., McGuigan, P. and Biewener, A. A. (2005). Patterns of strain and activation in the thigh muscles of goats across gaits during level locomotion. *J. Exp. Biol.* **208**, 4599-4611.
- Henry, H. T., Ellerby, D. J. and Marsh, R. L. (2005). Performance of guinea fowl *Numida meleagris* during jumping requires storage and release of elastic energy. *J. Exp. Biol.* **208**, 3293-3302.
- Herring, S. W., Grimm, A. F. and Grimm, B. R. (1979). Functional heterogeneity in a multipinnate muscle. *Am. J. Anat.* **154**, 563-576.
- Herzog, W. and Leonard, T. R. (1991). Validation of optimization models that estimate the forces exerted by synergistic muscles. *J. Biomech.* **24**, 31-39.
- Higham, T. E. (2007). Feeding, fins and braking maneuvers: locomotion during prey capture in centrarchid fishes. *J. Exp. Biol.* **210**, 107-117.
- Higham, T. E. and Jayne, B. C. (2004a). *In vivo* muscle activity in the hindlimb of the arboreal lizard, *Chamaeleo calyptratus*: general patterns and effects of incline. *J. Exp. Biol.* **207**, 249-261.
- Higham, T. E. and Jayne, B. C. (2004b). Locomotion of lizards on inclines and perches: hindlimb kinematics of an arboreal specialist and a terrestrial generalist. *J. Exp. Biol.* **207**, 233-248.
- Higham, T. E. and Nelson, F. E. (in press). The integration of lateral gastrocnemius muscle function and kinematics in running turkeys. *Zoology*.
- Higham, T. E., Biewener, A. A. and Wakeling, J. M. (2008). Functional diversification within and between muscle synergists during locomotion. *Biol. Lett.* **4**, 41-44.
- Hill, A. V. (1938). The heat of shortening and the dynamic constants of muscle. *Proc. R. Soc. Lond. B Biol. Sci.* **126**, 136-195.
- Hodgson, J. A. (1983). The relationship between soleus and gastrocnemius muscle activity in conscious cats – a model for motor unit recruitment? *J. Physiol.* **337**, 553-562.
- Hoyt, D. F., Wickler, S. J., Biewener, A. A., Cogger, E. A. and De Le Paz, K. L. (2005). *In vivo* muscle function vs speed. I. Muscle strain in relation to length change of the muscle-tendon unit. *J. Exp. Biol.* **208**, 1175-1190.
- Hutchinson, J. R., Schwerda, D., Famini, D. J., Dale, R. H. I., Fischer, M. S. and Kram, R. (2006). The locomotor kinematics of Asian and African elephants: changes with speed and size. *J. Exp. Biol.* **209**, 3812-3827.
- Irschick, D. J. and Jayne, B. C. (1999). Comparative three-dimensional kinematics of the hindlimb for high-speed bipedal and quadrupedal locomotion of lizards. *J. Exp. Biol.* **202**, 1047-1065.
- Jayne, B. C. and Irschick, D. J. (1999). Effects of incline and speed on the three-dimensional hindlimb kinematics of a generalized iguanian lizard (*Dipsosaurus dorsalis*). *J. Exp. Biol.* **202**, 143-159.
- Josephson, R. K. (1997). Power output from a flight muscle of the bumblebee *Bombus terrestris*. II. Characterization of the parameters affecting power output. *J. Exp. Biol.* **200**, 1227-1239.
- Kanda, K. and Hashizume, K. (1992). Factors causing difference in force output among motor units in the rat medial gastrocnemius-muscle. *J. Physiol. Lond.* **448**, 677-695.
- Katz, B. (1939). The relation between force and speed in muscular contraction. *J. Physiol.* **96**, 45-64.
- Kaya, M., Leonard, T. and Herzog, W. (2003). Coordination of medial gastrocnemius and soleus forces during cat locomotion. *J. Exp. Biol.* **206**, 3645-3655.
- Lammers, A. R., Earls, K. D. and Biknevicius, A. R. (2006). Locomotor kinetics and kinematics on inclines and declines in the gray short-tailed opossum *Monodelphis domestica*. *J. Exp. Biol.* **209**, 4154-4166.
- Lichtwark, G. A., Bougoulas, K. and Wilson, A. M. (2007). Muscle fascicle and series elastic element length changes along the length of the human gastrocnemius during walking and running. *J. Biomech.* **40**, 157-164.
- Marey, E. J. (1901). *Animal Mechanism: A Treatise on Terrestrial and Aerial Locomotion*. New York: D. Appleton.
- Marsh, R. L., Ellerby, D. J., Carr, J. A., Henry, H. T. and Buchanan, C. I. (2004). Partitioning the energetics of walking and running: swinging the limbs is expensive. *Science* **303**, 80-83.
- Marsh, R. L., Ellerby, D. J., Henry, H. T. and Rubenson, J. (2006). The energetic costs of trunk and distal-limb loading during walking and running in guinea fowl *Numida meleagris*. I. Organismal metabolism and biomechanics. *J. Exp. Biol.* **209**, 2050-2063.
- McGowan, C. P., Baudinette, R. V., Usherwood, J. R. and Biewener, A. A. (2005). The mechanics of jumping versus steady hopping in yellow-footed rock wallabies. *J. Exp. Biol.* **208**, 2741-2751.
- McGowan, C. P., Baudinette, R. V. and Biewener, A. A. (2007). Modulation of proximal muscle function during level versus incline hopping in tammar wallabies (*Macropus eugenii*). *J. Exp. Biol.* **210**, 1255-1265.
- McMahon, T. A. (1984). *Muscles, Reflexes, and Locomotion*. Princeton: Princeton University Press.
- Minetti, A. E., Ardigo, L. P., Reinach, E. and Saibene, F. (1999). The relationship between mechanical work and energy expenditure of locomotion in horses. *J. Exp. Biol.* **202**, 2329-2338.
- Morgan, D. L. (1985). From sarcomeres to whole muscles. *J. Exp. Biol.* **115**, 69-78.
- Mu, L. and Sanders, I. (2001). Neuromuscular compartments and fiber-type regionalization in the human inferior pharyngeal constrictor muscle. *Anat. Rec.* **264**, 367-377.
- Nelson, F. E. and Jayne, B. C. (2001). The effects of speed on the *in vivo* activity and length of a limb muscle during the locomotion of the iguanian lizard *Dipsosaurus dorsalis*. *J. Exp. Biol.* **204**, 3507-3522.
- Nelson, F. E. and Roberts, T. J. (2008). Task-dependent force sharing between muscle synergists during locomotion in turkeys. *J. Exp. Biol.* **211**, 1211-1220.
- Nishikawa, K. C., Biewener, A. A., Aerts, P., Ahn, A. N., Chiel, H. J., Daley, M. A., Daniel, T. L., Full, R. J., Hale, M. E., Hedrick, T. L. et al. (2007). Neuromechanics: an integrative approach for understanding motor control. *Integr. Comp. Biol.* **47**, 16-54.
- Pappas, G. P., Asakawa, D. S., Delp, S. L., Zajac, F. E. and Drace, J. E. (2002). Nonuniform shortening in the biceps brachii during elbow flexion. *J. Appl. Physiol.* **92**, 2381-2389.
- Peres-Neto, P. R., Jackson, D. A. and Somers, K. M. (2003). Giving meaningful interpretation to ordination axes: assessing loading significance in principal component analysis. *Ecology* **84**, 2347-2363.
- Pettigrew, J. B. (1874). *Animal Locomotion or Walking, Swimming and Flying with a Dissertation on Aeronautics*. New York: D. Appleton.
- Pierotti, D. J., Roy, R. R., Gregor, R. J. and Edgerton, V. R. (1989). Electromyographic activity of cat hindlimb flexors and extensors during locomotion at varying speeds and inclines. *Brain Res.* **481**, 57-66.
- Powell, P. L., Roy, R. R., Kanim, P., Bello, M. A. and Edgerton, V. R. (1984). Predictability of skeletal muscle tension from architectural determinations in guinea pig hindlimbs. *J. Appl. Physiol.* **57**, 1715-1721.
- Priulitsky, B. I., Herzog, W. and Allinger, T. L. (1996). Mechanical power and work of cat soleus, gastrocnemius and plantaris muscles during locomotion: possible functional significance of muscle design and force patterns. *J. Exp. Biol.* **199**, 801-814.
- Rassier, D. E., Herzog, W., Wakeling, J. and Syme, D. A. (2003). Stretch-induced, steady-state force enhancement in single skeletal muscle fibers exceeds the isometric force at optimum fiber length. *J. Biomech.* **36**, 1309-1316.
- Rice, W. R. (1989). Analyzing tables of statistical tests. *Evolution* **43**, 223-225.
- Roberts, T. J. (2001). Muscle force and stress during running in dogs and wild turkeys. *Bull. Mus. Comp. Zool.* **156**, 283-295.
- Roberts, T. J. and Marsh, R. L. (2003). Probing the limits to muscle-powered accelerations: lessons from jumping bullfrogs. *J. Exp. Biol.* **206**, 2567-2580.
- Roberts, T. J., Marsh, R. L., Weyland, P. G. and Taylor, C. R. (1997). Muscular force in running turkeys: the economy of minimizing work. *Science* **275**, 1113-1115.
- Roberts, T. J., Higginson, B. K., Nelson, F. E. and Gabaldon, A. M. (2007). Muscle strain is modulated more with running slope than speed in wild turkey knee and hip extensors. *J. Exp. Biol.* **210**, 2510-2517.
- Rubenson, J., Henry, H. T., Dimoulas, P. M. and Marsh, R. L. (2006). The cost of running uphill: linking organismal and muscle energy use in guinea fowl (*Numida meleagris*). *J. Exp. Biol.* **209**, 2395-2408.
- Scholle, H. C., Schumann, N. P., Biedermann, F., Stegeman, D. F., Grabme, R., Roeleveld, K., Schilling, N. and Fischer, M. S. (2001). Spatiotemporal surface EMG characteristics from rat triceps brachii muscle during treadmill locomotion indicate selective recruitment of functionally distinct muscle regions. *Exp. Brain Res.* **138**, 26-36.
- Soman, A., Hedrick, T. L. and Biewener, A. A. (2005). Regional patterns of pectoralis fascicle strain in the pigeon *Columba livia* during level flight. *J. Exp. Biol.* **208**, 771-786.
- Taylor, C. R., Heglund, N. C. and Maloij, G. M. O. (1982). Energetics and mechanics of terrestrial locomotion. I. Metabolic energy consumption as a function of speed and body size in birds and mammals. *J. Exp. Biol.* **97**, 1-21.

- Van Bavel, H., Drost, M. R., Wielders, J. D., Huyghe, J. M., Huson, J. M. and Janssen, J. D.** (1996). Strain distribution on rat medial gastrocnemius (MG) during passive stretch. *J. Biomech.* **29**, 1069-1074.
- Walmsley, B., Hodgson, J. A. and Burke, R. E.** (1978). Forces produced by medial gastrocnemius and soleus muscles during locomotion in freely moving cats. *J. Neurophysiol.* **41**, 1203-1216.
- Wang, L. and Kernell, D.** (2000). Proximo-distal organization and fibre type regionalization in rat hindlimb muscles. *J. Muscle Res. Cell Motil.* **21**, 587-598.
- Wang, L. and Kernell, D.** (2001). Quantification of fibre type regionalisation: an analysis of lower hindlimb muscles of the rat. *J. Anat.* **198**, 295-308.
- Wickler, S. J., Hoyt, D. F., Biewener, A. A., Cogger, E. A. and De Le Paz, K. L.** (2005). *In vivo* muscle function vs speed. II. Muscle function trotting up an incline. *J. Exp. Biol.* **208**, 1191-1200.
- Zajac, F. E.** (1989). Muscle and tendon: properties, models, scaling, and application to biomechanics and motor control. *Crit. Rev. Biomed. Eng.* **17**, 359-411.
- Zar, J. H.** (1996). *Biostatistical Analysis*. Upper Saddle River, NJ: Prentice Hall.